Hourly air temperature forecasting by downscaling WRF simulations over complex topography: A case study of Chongli District in Hebei Province, China

Guangxing Zhang[1], Shanyou Zhu[1], Nan Zhang[2], Guixin Zhang[1], and Yongming Xu[1]

[1]Nanjing University of Information Science and Technology
[2]Hebei Meteorological Observatory

November 22, 2022

Abstract

Accurate and high-resolution air temperature prediction is important in many different applications. Hourly air temperature forecasting in mountainous areas is necessary and important because mountainous areas are becoming increasingly important areas of human activities. At present, scientists successfully employ numerical weather prediction (NWP) models, such as the WRF model, to achieve reliable forecasts. However, air temperature forecasting and modeling over complex geographical zones are difficult tasks. The WRF model is a mesoscale model and does not adequately account for the influence of terrain on the air temperature. It is important to downscale larger-scale models to a much finer scale. In this paper, a statistical temperature downscaling method based on geographically weighted regression (GWR) and diurnal temperature cycle (DTC) models is proposed. A statistical downscaling scheme is designed to forecast the hourly air temperature, at a 30-m spatial resolution, up to 24 h in advance. Compared to WRF simulations, RMSE of the combined downscaling model decreased 1.01 at the automatic weather station level and 0.80 at the spatial level, and MAE decreased by 0.81 and 0.69 , respectively, at these two levels. The results reveal that the combined downscaling model performs very well in correcting and downscaling the air temperature in WRF simulations in mountainous areas.

Hosted file

`essoar.10507609.1.docx` available at https://authorea.com/users/534129/articles/598398-hourly-air-temperature-forecasting-by-downscaling-wrf-simulations-over-complex-topography-a-case-study-of-chongli-district-in-hebei-province-china

Hourly air temperature forecasting by downscaling WRF simulation over complex topography: A case study of Chongli District in Hebei Province China

Guangxing Zhang[a], Shanyou Zhu[a,*], Nan Zhang[b], Guixin Zhang[c], Yongming Xu[a]

[a] School of Remote Sensing and Geomatics Engineering, Nanjing University of Information Science & Technology, Nanjing 210044, China

[b] Hebei Meteorological Observatory, Shijiazhuang 050021, China

[c] School of Geographical Sciences, Nanjing University of Information Science & Technology, Nanjing 210044, China

Abstract

The accurate and high-resolution prediction of air temperature is important in many different applications. Hourly air temperature forecasting in mountain area is necessary and important because mountain area is becoming an important area of human activity. At present scientists are successfully using Numerical Weather Prediction (NWP) models, such as WRF, to achieve a reliable forecast. However, air temperature forecasting and modeling over complex geographical zones are difficult, WRF is a mesoscale model and not adequately account for the influence of terrain on air temperatures. It is important to downscale from larger scale models to a much finer scale. In this paper, a statistical temperature downscaling method based on geographically weighted regression (GWR) and diurnal temperature cycle (DTC) model is proposed. The statistical downscaling scheme was designed to forecast hourly air temperature, with 30-m spatial resolution, up to 24 h in advance. Compare to WRF simulation, RMSE of combined downscaling model decreased 1.01 ℃ at automatic weather stations level and 0.80 ℃ at spatial level, and MAE decreased by 0.81 ℃ and 0.69 ℃ at two levels, respectively. The results reveal that the combined downscaling model performance very well to correct and downscaling air temperature of WRF simulation in mountain area.

Keywords

air temperature forecasting; WRF; diurnal temperature cycle; Geographically Weighted Regression (GWR); statistical downscaling; bias correction; mountain area

1. Introduction

Air temperature is one of the most measured meteorological parameters. Air temperature forecasting has been a crucial climatic factor required for many different applications in areas such as agriculture, industry, energy, environment, tourism, etc. (Abdel-Aal 2004; Cifuentes et al., 2020). Some of these applications include short-term load forecasting for power utilities (Li et al., 2016), protection against freezing injury of fruits (Chung et al., 2006), adaptive temperature control in greenhouses (Dombaycı and Gölcü, 2009), prediction of cooling and energy consumption in residential buildings (Ben-Nakhi and Mahmoud, 2004), and establish a planning horizon for infrastructure upgrades, insurance, energy policy, and business development (Smith et al., 2007). Therefore, accurate forecast of air temperature with higher spatio-temporal resolution has always been an important goal for the meteorologists and weather forecasters.

Nowadays, many Numerical weather prediction (NWP) models are available for air temperature prediction; e.g., the European Centre for Medium-Range Weather Forecasts (ECMWF) model, the fifth-generation mesoscale model (MM5), and the Weather Research and Forecasting (WRF) model. All these NWP models allow day-ahead air temperature prediction, which is usually adopted in practice. However, uncertainties from model inputs, model parameter estimation, and the model structure are unavoidable in NWP modeling. These uncertainties make it difficult for the accuracy of NWP models used in air temperature prediction to meet the increasing needs of grid systems (Xu et al., 2021). Meanwhile, due to their coarse spatial resolution, mostly lower than 1km (Caldwell et al., 2009; Yan et al., 2020), NWP is mainly used for developing climate change scenarios and for large scale studies. Obviously, this kind of model cannot be used to represent climate variability at the local scale, such as in vineyard areas and mountain areas, so it is important to downscale from larger scale models to a much finer scale in order to investigate climate variability at a more appropriate resolution (Cheng et al., 2008; Le Roux et al., 2018).

Mountain area is also an important area of human activity, such as fruit planting, tourism, skiing in winter season. So hourly air temperature forecasting in mountain area is necessary and important. Meanwhile high-resolution air temperature is also very important. Unlike the plain areas, the topography of the mountain area is very complex. Complex terrain can cause air temperature to change in a smaller terrain unit. In a 1-km grid, assuming that the slope of the grid is 0.5, the difference of altitude at the top and foot of the slope can be as much as 500m, and the temperature difference can be as high as 3℃. Air temperature forecasting and modeling over complex geographical zones are difficult, because temperature is influenced by several nonlinear processes such as the interaction of large-scale circulation of air masses with local air flows, airflow-topography interaction, and the interplay between radiation and topographic shading, among others.

As a result, a variety of techniques, such as downscaling methods, have been developed to bridge the gap between the scale at which data is available and the scale at which it is needed for assessment. Downscaling methods can be split into two broad groups: dynamical downscaling and statistical downscaling. One of the main issues for dynamical downscaling is the large amount of computing time needed to achieve fine scale resolution. It's essential to improve the resolution of climate model without increasing the resources required in the modelling process. Statistical downscaling uses observed relationships between variables at different spatial scales to predict regional-scale model fields from coarser data (Caldwell et al., 2009; Le Roux et al., 2018). Compared to other downscaling methods (e.g. dynamical downscaling), the statistical method is relatively easy to use and provides station-scale climate information from NWP output (Wilby et al., 2002; Cheng et al., 2008). It has been shown that the statistical method has comparable accuracy to that of dynamical downscaling (Schoof and Pryor, 2001). Spatial interpolation methodologies, such as inverse distance weighted (IDW) method and kriging techniques, are now widely used for statistical downscaling. However, large uncertainties arise when applying them to complex-terrain areas (Jiang et al., 2021), while the geographically weighted regression (GWR) method is more effective when analyzing the nonstationary spatial parameters and is widely used (Zhou et al., 2019).

Although there have been many studies on statistical downscaling, most of the previous studies focused only on daily and monthly air temperature downscaling (Cheng et al., 2008). For example, some studies have studied downscale of daily mean air temperature (Hofer et al., 2015, Wang et al., 2020), daily minimum air temperature (Holden et al., 2011) and maximum air temperature (Wang et al., 2020; Viggiano et al., 2019). To better extend climate change impacts analysis in estimates of future synoptic weather types and meteorological variables, not only daily, but also hourly, climate scenarios are necessary. There have been studies on hourly air temperature forecasting in urban area (Yi et al., 2018), however, rarely studies in mountain areas. Despite the above uncertainty, it has been shown that regression functions can be used to represent the relationship between temperature and terrain (Schoof and Pryor, 2001). Therefore, in order to achieve the purpose of downscaling, we can use high-resolution terrain data to improve the spatial resolution of WRF data by constructing the relationship between air temperature and terrain.

In order to obtain hourly temperature, air diurnal temperature cycle (DTC) model is an effective method. Maximum and minimum air temperature with some other parameters, such as hourly air temperature, could be estimated by DTC, as a parametric method (Duan et al., 2012; Gholamnia et al., 2017; Hu et al., 2020). The DTC model can be used to improve inputs for numerical weather models or assimilated data (Gholamnia et al., 2019). The shape of the diurnal temperature curves has been modeled in a variety of ways that vary from simple curve-fitting models based upon sine curves to more sophisticated techniques utilizing Fourier analysis and complex energy balance models (Reicosky et al., 1989; Gholamnia et al., 2019). Therefore, the DTC model can be constructed by observation data of weather station, and then build multiple linear regression model between DTC model coefficients and local parameters, such as altitude, slope, and aspect, etc. Through this process, high spatial resolution hourly forecasts were then obtained by stretching/contracting this DTC model.

The statistical downscaling scheme in this study was designed to forecast hourly air temperature, with 30-m spatial resolution, up to 24 h in advance in a mountain area from WRF. This study develops a multi-step downscaling and correction model to improve WRF performance on air temperature prediction. The steps are as follows: 1) build DTC model of with observation data from automatic weather stations (AWSs) and determine how to use the DTC in forecast; 2) downscaling WRF air temperature at the height of 2-m with the spatial resolution of 1 km to 30-m via GWR method; 3) correct daily mean air temperature of WRF downscaling results combined with ground observation data; 4) used multiple linear regression to spatialization the daily mean air temperature correction model and the DTC model; 5) combined with the downscaling results via GWR, the spatialized multiplicative correction model, and the spatialized DTC model to predict air temperature of the study area.

2. Study area and data

2.1 Study area

This study area is in Chongli District, Zhangjiakou City, Hebei Province of China (Fig. 1), and covers around 2300 km^2. The bounding coordinates of the study area are 114.8°-115.6°E, 40.8°-41.3°N. This area belongs to a semi-arid monsoon climate zone. The complex terrain of Chongli District has an elevation range from about 812 m to about 2169 m, with a mean elevation of 1485 m.The study area is one of the venues for the 2022 Beijing Winter Olympic Games. In the future, the region will be a hot spot of tourism and sports. Therefore, providing correct and high spatial and temporal resolution air temperature forecast in this area is quite necessary.

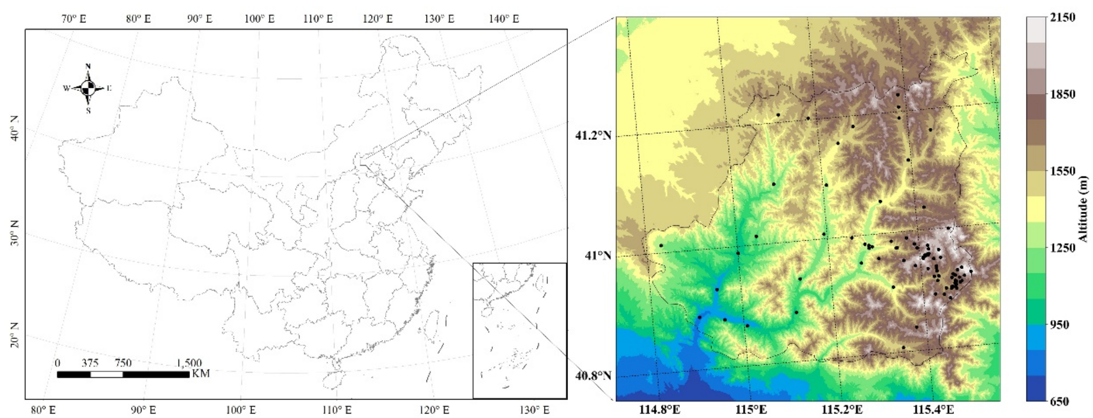

Fig. 1. Elevation diagram of the simulation area. The distribution of 76 automatic weather stations (AWSs) is shown by black dots.

2.2. ASTER DEM

In this study, ASTER DEM was used to get 30-m resolution altitude of the whole study area, and to calculate slope and aspect. The ASTER DEM version 2 is a global one arc-second elevation dataset that was released in October 2011 by METI, Japan and NASA. The ASTER DEM was generated using optical imagery of 15 m resolution collected in space with the METI ASTER sensor mounted on NASA's Terra satellite (Abrams et al., 2010). The sensor has three spectral bands in the visible infrared spectrum, six bands in the short wavelength infrared spectrum as well as in the thermic infrared spectrum. The first, 1 Arc second (~30-m) GDEM1 was released in June 2009 and covered the globe from 83° N latitude to 83° S latitude. GDEM1 was derived from approximately 1.2 million images and had a vertical accuracy of 20 m at the 95% confidence level (ASTER GDEM Validation Team, 2009).

2.3. WRF simulations

The WRF model is a numerical weather prediction model for mesoscale weather systems developed by the United States for simulation and real-time forecasting. It uses scale analysis to solve fluid dynamics and thermodynamic equations that express atmospheric motion in predicting the future atmospheric circulation and weather (Xu et al., 2021).

In this study, the WRF version 3.7.1 with the center located at 108° E, 38° N was configured with three domains at 9km, 3km and 1km horizontal resolutions, respectively. The model's vertical resolution was discretized with 50 full terrain-following levels with the model top at 50 hPa for all domains. There are 550 grid points in the east-west and 484 grid points in the north-south directions for Domain 03 (d03). The National Centers for Environmental Prediction (NCEP) Global Forecast System (GFS) Final (FNL) operational global analyses of 0.5° resolution was used for initial conditions with ingestion every 6 h. Each episode is initialized at 12:00 UTC and it is independently run-in periods of 36 h. The first six hours are considered as spin-up time. The various physical parameterization options utilized in the present study are as follows: the Thompson parametrization is chosen for the microphysics; the Yonsei University (YSU) as the Planetary Boundary Layer (PBL) scheme; the RRTM longwave scheme and the Dudhia shortwave scheme are used for radiation; finally, the Noah land-surface model is used as the surface layer scheme. The time range of the simulation data is from January 15, 2020 to January 19, 2020, a total of five days.

2.4. Ground Observation data

Observed hourly 2-m air temperature at 76 automatic weather stations (AWSs) (see Fig. 1) in Chongli District, Zhangjiakou City, Hebei Province of China are used in this study. These observations are part of records from gradually evolving AWSs that are owned and maintained by the Hebei Meteorological Administration. These stations are located at an average altitude of about 1500 m. These data were reviewed through a quality control procedure to identify any invalid values and missing data.

3 Methods

Fig. 2 summarizes the overall procedure we followed in this study. As shown in Fig. 2, firstly, downscaling WRF air temperature to 30-m spatial resolution via geographically weighted regression (GWR) method, where, WRF simulation air temperature is dependent variable, aspect, slope, and altitude are independent variables. Then, combined with ground observation data to build daily air temperature cycle (DTC) model, and used multiple linear regression to spatialization the DTC model. Next, combined with ground observation data to correct the downscaled WRF simulation daily mean air temperature and used multiple linear regression to spatialization the correction model. Finally, combined with the downscaling results, the spatialized correction model, and the spatialized DTC model to predict air temperature of the study area. Every step in Fig. 2 is described in details below.

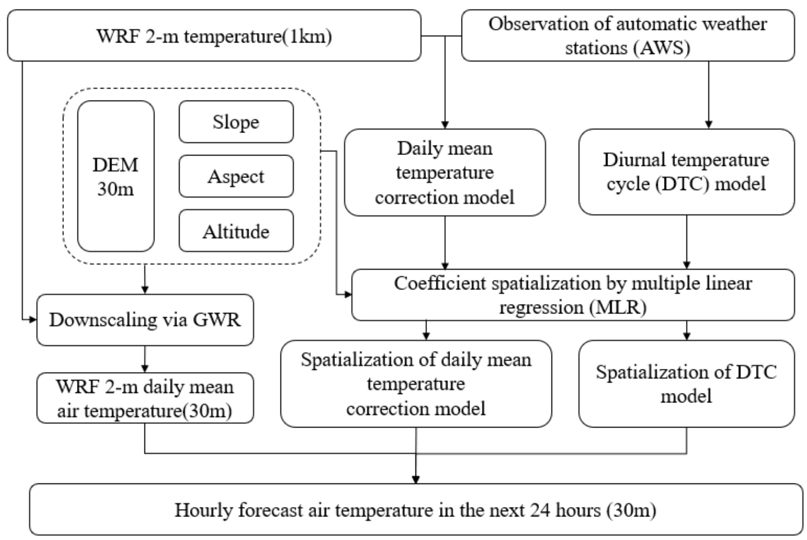

Fig. 2. The flow chart of this study.

3.1 Geographically weighted regression method

In this study, geographically weighted regression (GWR) was used to downscale WRF air temperature and spatial interpolation of observation data which was used to compare results of downscaling and WRF simulation. The GWR is a local modeling technique appropriate for spatial data with some degree of spatial dependence (Georganos et al., 2017). It effectively deals with the coexistence of spatial correlation and spatial heterogeneity. GWR model is looking for determine the existence of spatial non-stationarity between a dependent variable and set of independent variables (Khosravi et al., 2017). GWR calculates regression coefficients at each individual location towards the ordinary least squares (OLS) model that calculates the coefficients for the whole study area (Fotheringham et al., 1997). The GWR model is expressed as:

$y(m) = \beta_0 + \sum_{k=1}^{p} \beta_k x_k(m) + \varepsilon(m)$ (1)

where $y(m)$ is the value of the response variable y at location m; x_k is the value of the kth independent variable; β_0 is the regression constant; β_k is the correlation coefficient for the independent predictor variable x_k; and $\varepsilon(m)$ is the random error term association with location m (Fotheringham et al., 2016). In this study, the response variable is air temperature, and the independent variables are slope, aspect, and altitude.

3.2 Air diurnal temperature cycle model

According to the Fourier series theory, a complex periodic function or periodic sequence is formed by the superposition of sine waves with different amplitudes and phases. Air diurnal temperature cycle (DTC) model is based on this method of extracting known periodic changes of elements and analyzing the law of sequence changes. DTC model has been widely applied to capture key diurnal characteristics, e.g., daily maximum, with a high degree of accuracy, and other applications, such as cloud screening, emissivity estimations, and capturing diurnal patterns of urban heat islands over a short time period (Duan et al., 2014, Zhou et al., 2013). DTC model is often used to fit and repair historical data, but rarely for temperature forecast. In this paper, we try to use this model to forecast air temperature.

We used the Fourier Transform method to convert diurnal temperature variation into a set of harmonics (Wang et al., 2018). Periodic air temperature variation can be transformed into the sum of harmonics with different frequencies, as follows:

$T(t) = \overline{T} + \sum_{k=1}^{M} \widetilde{T}_k \sin(\omega_k t + \varphi_k)$ (2)

where, $T(t)$ is the air temperature of time t, t is the local solar time of a day and its value range 0-23, $\overline{T}$ is the daily mean temperature, M is the order of Fourier function, $\widetilde{T}$ is the amplitude, φ is the phase and $\omega = 2\pi/P$ is the fundamental angular frequency, with the period P equals 24 hours for the daily cycle.

For daily air temperature cycle, daily and semi-daily harmonics representing the fundamental periodic variation. The strong signal for the daily harmonics reflects the primary forcing mechanism, solar radiation. The semi-daily cycle is mainly imposed by the abrupt night-time zeroing of solar radiation in addition to the heat storage of the soil and atmosphere. The observations for a day can be treated as two periodic variations and other random variations, as follows:

$T(t) = \overline{T} + \widetilde{T}_{d1} \sin(\frac{2\pi}{24}t + \varphi_{d1}) + \widetilde{T}_{d2} \sin(\frac{2\pi}{12}t + \varphi_{d2})$ (3)

The major parameters are the daily mean temperature $\overline{T}$, amplitude $\widetilde{T}_{\mathrm{di}}$ and phase φ_{di} of the daily harmonic (24-h harmonic, i=1) and the semi-daily cycle (12-h harmonic, i=2). φ can be calculated by the peak/bottom temperature occurring time. According to the statistical data of observation data, the harmonics performance best when set the peak temperature of the study area in a daily cycle occurs at 14:00 and bottom temperature occurs at 7:00. All the harmonic functions of 76 AWSs of previous day were built via curve fitting.

In order to apply harmonics to air temperature forecast, the next day's mean temperature and amplitude $\widetilde{T}_{\mathrm{di}}$ are key parameters. Excluding the daily mean temperature from the harmonics, the rest of the harmonics represents the variation of temperature difference between the daily mean temperature and temperature of each local solar time. Through experiment, the temperature difference of next day can be better predicted by multiplying the harmonics of the previous day by a scaling factor. The scaling factor would be adjusted as follows:

$r = \frac{\overline{T}_f}{\overline{T}_o}$ (4)

Where, $\overline{T}$ is mean air temperature, f forecast day, and o is observation of previous day.

However, the daily mean air temperature of forecast day is unknown when to forecast air temperature. In this study we tried to use daily mean temperature of WRF simulation as the daily mean air temperature of forecast day. It will lead to a large error in the result if daily mean air temperature of WRF simulation is directly used, because there is random error of WRF simulation. So, we first revised the WRF daily mean air temperature using the following correction method.

3.3 Multiplicative correction for WRF simulation

The daily mean temperature of forecast day is the key variable when use DTC model to forecast air temperature. Bias correction of WRF is a useful method to get daily mean temperature of forecast day. Error correction models have been developed to improve the accuracy of numerical output by training the relationship between prediction errors and related variables (Xu et al., 2021). Application of bias correction techniques has become increasingly popular to perform local correction of the deterministic model outputs with empirical formulae. These empirical formulae include additive correction (mean bias subtraction), multiplicative correction, hybrid model, model output statistics (MOS), and Kalman filter-based correction (Mok et al., 2017). The additive correction adjusts the forecast for a particular monitoring station by adding the temporal average of the measured biases during the previous days to the forecast of the deterministic model (Monteiro et al., 2013; Wilczak et al., 2006), while the multiplicative correction is performed by multiplying a ratio to the forecast (Borrego et al., 2011; Monteiro et al., 2013). This ratio is obtained from dividing the sum of observed concentrations at the station during the past few days by the sum of the forecasted concentrations of the deterministic model during the same period. The hybrid forecast is a special case of the additive correction, which only uses the bias of the previous day to perform correction (Neal et al., 2014; Silibelo et al., 2015). For MOS, a correction model based on linear regression is generated between the measured pollutant concentration and the forecast (Monteiro et al., 2013) or a set of independent variables such as meteorological measurements (with their respective parameters) (Konovlav et al., 2009), and is applied to the posterior processing after trained with historical data. Kalman filter based bias correction, the additive and the multiplicative model biases are estimated adaptively at each time step based on the weighted combination between the prior estimates and the contribution from the new measurement (Borrego et al., 2011).

Multiplicative correction, also called linear correction, is a simple bias-correction technique. It uses a scaling factor between the observations and the simulation in the calibration period to reduce the future bias (Ines and Hansen, 2006). In this method, assuming that the ratios between field measurement (observation) and WRF simulation of the previous day and the forecast day are the same, then air temperature of next day can be corrected by the ratio of the previous day. The forecast air temperature corrected from WRF simulation would be adjusted as follows:

$$\widetilde{T} = \frac{\sum_{i=1}^{n} T_o}{\sum_{i=1}^{n} T_m} \times T_{m-f} \quad (5)$$

where T is the air temperature of either observation (o) or model (m) for a historic training period, f means the forecast day, n represents the number of days of historical data.

In this paper, we used the equation (5) to correct the WRF mean air temperature. So, T_o was replaced by mean air temperature of historical data of AWSs, T_m was replaced by mean air temperature of historical data of WRF, and T_{m-f} was replaced by mean air temperature of forecast data of WRF. All the WRF value used in here was downscaling results via GWR. In this study as the nearest grid point of WRF value is forecast value of AWSs.

As the WRF daily mean air temperature calculated via equation (5) is the daily mean temperature of forecast day. Combine the equations (3), (4), and (5), the forecast equation would be adjusted as follows:

$$T(t) = \frac{\sum_{i=1}^{n} \overline{T}_o}{\sum_{i=1}^{n} \overline{T}_m} \times \overline{T}_{m-f} \{1 + \frac{1}{\overline{T}_o} \times (\widetilde{T}_{d1} \sin(\frac{2\pi}{24} t + \varphi_{d1}) + \widetilde{T}_{d2} \sin(\frac{2\pi}{12} t + \varphi_{d2}))\} \quad (6)$$

where, t is local solar time, range from 0 to 23, T is forecast temperature.

3.4 Spatialization of DTC model and daily mean air temperature correction model

All the above models are based on observation data and WRF simulation of AWSs. They can only forecast temperature at AWSs. It is not enough to correct and downscale at AWSs, the goal is to make a spatial prediction for the entire study area. Therefore, the DTC model and daily mean air temperature correction model need spatialization. For spatialization, spatial interpolation methodologies are widely used, such as inverse distance weighted (IDW) method and kriging techniques. However, large uncertainties arise, and most of WRF grids are not used properly when applying them to complex-terrain areas. Although there is bias in WRF simulation, the result of interpolation is not better than that of WRF. Therefore, all grid data of WRF need to be corrected before forecasting in the entire study area. At the same time, DTC model of AWSs were also need to be spatialized. Then, the air temperature at each moment of the entire study area can be predicted in the forecast day.

As shown in formula (5), the formula can be divided into two parts, which the left part is a scaling factor calculated by the WRF and the observation data of the previous day. The scaling factor would be adjusted as follows:

$\alpha = \frac{\sum_{i=1}^{n} T_o}{\sum_{i=1}^{n} T_m}$ (7)

where α is correction coefficient for WRF simulation of next day.

It has been shown that regression functions can be used to represent the relationship between air temperature and terrain (Schoof and Pryor, 2001). Then we build a multiple linear regression for , where the   is dependent variable and altitude, slope, and aspect are independent variables. The   would be adjusted as follows:

$\alpha = a_1 H + a_2 S + a_3 A + b$ (8)

where, H is altitude, S is slope, and A is aspect of AWSs, a and b are the coefficients of the regression equation.

Through formula (8), bring independent variables of all grid of WRF into the formula, the corrected air temperature of all grid could be obtained. The corrected WRF data was used as the basic data for DTC model.

The multiple linear regression model for $\widetilde{T}_{\mathrm{di}}$ was also built, where the $\widetilde{T}_{\mathrm{di}}$ was dependent variable and altitude, slope, and aspect are independent variables. The $\widetilde{T}_{\mathrm{di}}$ would be adjusted as follows:

$\widetilde{T}_{\mathrm{di}} = c_{i1} H + c_{i2} S + c_{i3} A + d$ (9)

where, H is altitude of AWSs, c and d are the coefficients of the regression equation.

Then, air temperature spatial distribution of study area at each local solar time would be forecasted combine the above formula.

4. Results and discussion

4.1. DTC fit performance at AWSs

The DTC model can represent most of the daily variations, as shown in Fig. 3. The root-mean-square error (RMSE) between DTC model results and the observed data is 0.601℃ for daily cycle over all 76 AWSs. The mean RMSE histogram of all 76 AWSs shows that most RMSE is less than 1℃ and the mean RMSE of all stations in the five days is 1.03℃.

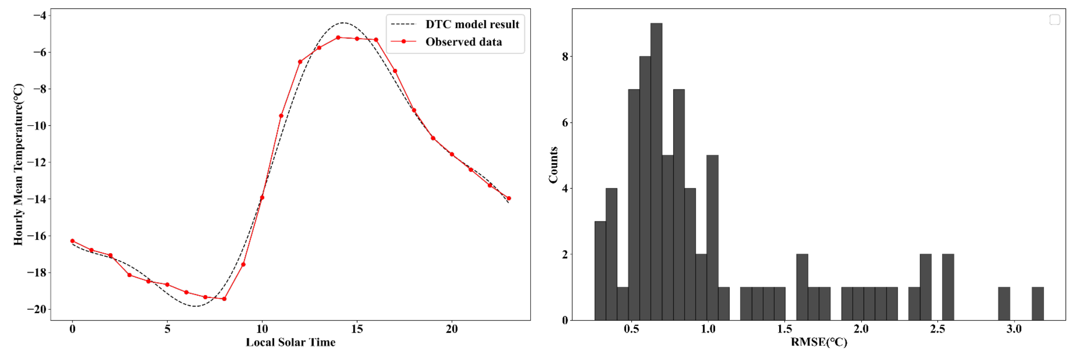

Fig. 3. DTC model and observed air temperature curve of all 76 AWSs hourly mean value (time range from 15 Jan to Jan 19, left side figure) and mean RMSE (between DTC model result and observed data, time range from 15 Jan to Jan 19) histogram of all 76 AWSs (right side figure).

Excluding the daily mean temperature from the DTC model, the rest of the DTC model represents the difference between daily mean temperature and temperature of each local solar time. The scatter for simulated temperature difference of four previous day against measured value of all AWSs can be seen in Fig. 4. Results show very high accuracy of reconstruction (R^2 >0.89) for air temperature difference. The distribution of DTC-simulated results can be observed as well-fitted to the one-to-one line. The DTC model has a very good performance on fit diurnal air temperature.

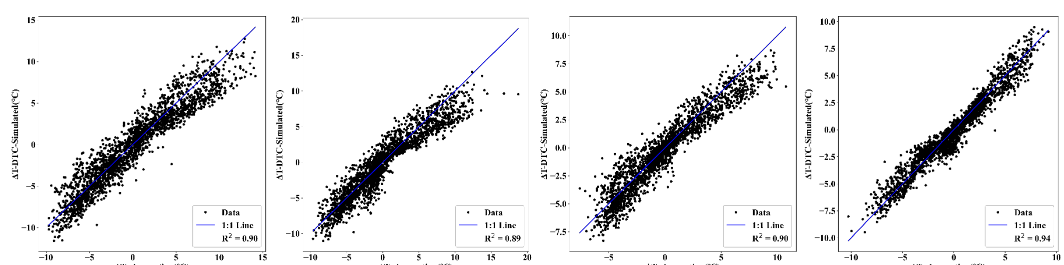

Fig. 4. Scatter plots for observation air temperature of AWSs (ΔT-observation) and DTC simulated air temperature (ΔT-DTC-Simulated) difference between hourly air temperature and daily mean temperature in model building day. (From left to right are the results of January 15, 16, 17 and 18, respectively.)

The DTC model was applied to forecast day, the performance can be seen in Fig. 5. In four forecasting day, all R^2 of DTC-simulated results is greater than 0.65. The distribution of DTC-simulated results can be observed as well-fitted to the one-to-one line, also. The DTC model has a very good performance on fit diurnal air temperature of forecast day. So, the downscaling model can be used to forecast and correct air temperature of forecast day.

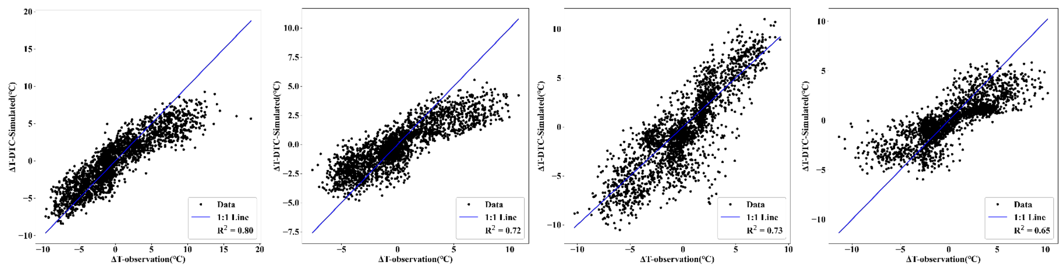

Fig. 5. Scatter plots for observation air temperature of AWSs (ΔT-observation) and DTC simulated air temperature (ΔT-DTC-Simulated) difference between hourly air temperature and daily mean temperature in model forecasting day. (From left to right are the results of January 16, 17, 18 and 19, respectively.)

4.2. Performance of multiplicative correction method at AWSs

In this paper, daily mean air temperature as the meteorological variable has been corrected. The corrected daily mean air temperature in the next 24 hours for all AWSs was calculated by formula (5). The accuracy of the corrected results was verified by the observation data. Root-mean-square error (RMSE) is calculated to assess the performance of the results. The smaller the value of RMSE, the more accurate the correction.

The original RMSE of WRF simulation (WRF-simulated) and RMSE of the multiplicative correction results (WRF-corrected) were calculated respectively. The results are shown in Table 1. With the increase of n, the result does not get better. Therefore, n set equals to one for the following research. So far, daily mean temperature used to predict next day's temperature has also been obtained.

Table 1

RMSE (℃) of WRF simulation (WRF-simulated) and multiplicative correction method results (WRF-corrected) (n represents the number of days of historical data)

Date	WRF-simulated	WRF-corrected			
		n=1	n=2	n=3	n=4
Jan 16	2.77	1.33	--	--	--
Jan 17	1.43	2.22	1.09	--	--
Jan 18	1.25	0.75	2.67	1.68	--
Jan 19	2.78	2.02	2.14	3.91	2.65
mean	2.06	1.58	1.97	2.79	2.65

4.3. Combined downscaling model performance against AWSs

The only unknown variable is daily mean temperature of forecast day when to forecast temperature of next day at AWSs. The daily mean temperature of forecast day will be obtained from WRF downscaling results via GWR. Combine GWR results, multiplicative correction model, and DTC model as combined model to predict air temperature of AWSs.

The predictive power of combined model is evaluated using the observation data set extract from AWSs, these all 76 stations data are not involved in building the model. Comparison of all the hourly values for all stations in four consecutive days (January 16, 2020 - January 19, 2020). The relationship between raw WRF simulation (WRF-simulated), combined model results (WRF-downscaled) and measured values of AWSs were compared. Three different statistical scores, among the most used accuracy measures, are calculated to assess the performance of the results. These are coefficient of determination(R^2), root-mean-square error (RMSE) and mean absolute error (MAE). The statistical results can be found in Table 2.

Table 2

WRF simulation (WRF-simulated) and combined model results (WRF-downscaled) performance statistics against ground station observation data over mean value of all AWSs.

Date	WRF-simulated		WRF-downscaled			
	R^2	*RMSE*	*MAE*	R^2	*RMSE*	*MAE*
Jan 16	0.51	3.61	2.70	0.79	2.73	2.36
Jan 17	0.42	2.79	2.42	0.87	1.79	1.59
Jan 18	0.47	2.80	2.40	0.60	1.94	1.68
Jan 19	0.71	3.20	3.02	0.75	1.92	1.65
mean	0.53	3.10	2.63	0.75	2.09	1.82

As expected, we see a significant increase in performance metrics for the combined model results to the WRF simulation. The R^2 value is significant higher from 0.53 to 0.75, the RMSE and MAE decreased by 1.01 ℃ and 0.81 ℃, respectively. The combined model has a good performance at AWSs for correction and downscaling of air temperature forecasting.

4.4 Downscaling model spatial uncertainty assessment

After verifying the correlation between AWSs, WRF simulation, and combined model results, we can investigate the spatial correlation between WRF simulation and combined model results where ground stations do not exist. For observation data of AWSs through GWR interpolation to get their spatial distributions (GWR-interpolation). In this section, the spatial distribution of WRF simulation (WRF-simulated), combined model results (WRF-downscaled), GWR-interpolation air temperature value, and their spatial bias are compared.

The spatial forecasting data was calculated by the combined model, which coefficients were spatialized already. The independent variables of the GWR downscaling model were obtained by DEM with 30-m resolution, so we can get the combined model results with 30-m spatial resolution. For spatial forecasting, 50 AWSs (about 2/3 of total) were selected to build the combined model, the other 26 stations (about 1/3 of total) were used to validate the combined model. RMSE of WRF-simulated and WRF-downscaled in four forecast days are shown in Fig. 6. The combined model has a better performance than raw WRF simulation. The WRF RMSE of January 16, 17, 18 and 19 is 3.90℃, 2.71℃, 2.42℃ and 3.29℃, respectively. Meanwhile, the combined model RMSE is 2.76℃, 2.03℃, 1.88℃ and 2.45℃, respectively. It has gone down 1.14℃, 0.68℃, 0.54℃ and 0.84℃, respectively. The RMSE of combined model decreased by an average of 0.8℃. For each local solar time, most of times the RMSE have decreased, only a few times have increased.

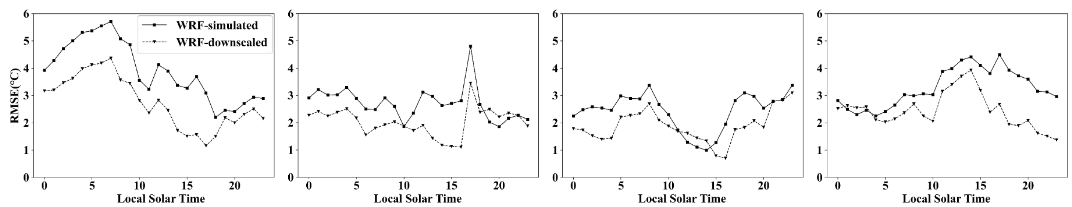

Fig. 6. RMSE of combined model results (WRF-downscaled) and WRF simulation (WRF-simulated) in four forecast days. (From left to right are the results of January 16, 17, 18 and 19, respectively.)

Then, 2000 random points were generated, and raw WRF simulation, combined model results and spatial measured values generated via GWR are extracted by these random points. Next, compare these data sets at four local solar times in a day, which are 02h, 08h, 14h and 20h, respectively. For each time, three statistical measures (R^2, RMSE, and MAE) were calculated as general performance metrics. From the statistical results (Table 3), we can find that R^2 of the combined model has a significant increase, except for a slight decrease in individual moments. The mean value of all times increased from 0.45 to 0.73. And, most of the time, RMSE and MAE have a significant decrease, the mean values are 2.26 ℃ and 1.96 ℃, respectively. Compared to WRF simulation, RMSE and MAE of combined model results decreased by 0.80 ℃ and 0.69 ℃, respectively.

Table 3

WRF simulation (WRF-simulated) and combined model results (WRF-downscaled) performance statistics against ground observation data at four different local solar times (02h, 08h, 14h and 20h) over mean value of random points.

Time	WRF-simulated		WRF-downscaled			
	R^2	RMSE	MAE	R^2	RMSE	MAE

Time	WRF-simulated		WRF-downscaled			
Jan 16-02h	0.43	3.19	2.62	0.76	1.93	1.54
Jan 17-02h	0.44	2.46	2.13	0.87	1.11	0.95
Jan 18-02h	0.55	1.93	1.54	0.68	2.18	1.81
Jan 19-02h	0.37	2.70	2.25	0.85	1.85	1.66
Jan 16-08h	0.40	3.77	3.18	0.89	4.16	3.94
Jan 17-08h	0.49	2.85	2.36	0.85	2.50	2.35
Jan 18-08h	0.19	3.94	3.43	0.42	2.21	1.78
Jan 19-08h	0.31	2.24	1.83	0.22	4.98	4.38
Jan 16-14h	0.66	3.78	3.48	0.52	3.50	2.90
Jan 17-14h	0.54	3.67	3.39	0.81	2.24	1.95
Jan 18-14h	0.45	1.87	1.52	0.63	1.85	1.56
Jan 19-14h	0.64	5.02	4.74	0.85	2.15	1.85
Jan 16-20h	0.63	1.81	1.52	0.92	1.33	1.09
Jan 17-20h	0.36	2.16	1.76	0.94	1.30	1.13
Jan 18-20h	0.46	3.56	3.13	0.64	1.90	1.60
Jan 19-20h	0.39	4.09	3.67	0.76	1.03	0.95

The scatter for WRF simulation (WRF-simulated) and combined model downscaling results (WRF-downscaled) of January 17 against GWR-interpolation air temperature value at four times can be seen in Fig. 7. The distribution of WRF-downscaled can be observed as well-fitted to the one-to-one line, but the distribution of WRF-simulated is not so well-fitted to the line, meanwhile R^2 of WRF-downscaled is greater than WRF-simulated also. The results show that the WRF-downscaled has a very good performance on correction and downscaling of forecast air temperature in this mountain area.

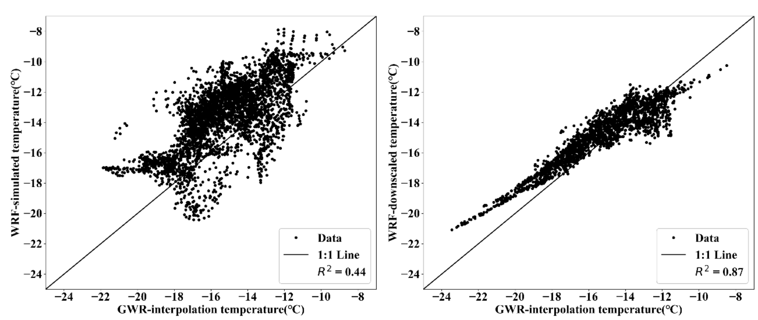

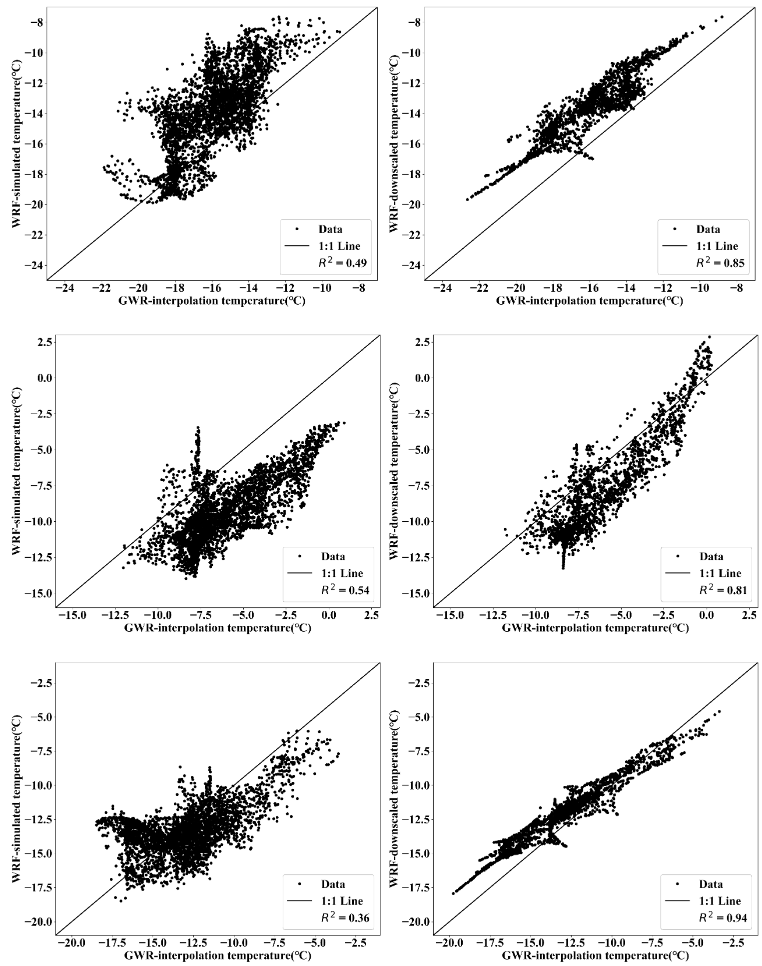

Fig. 7. Scatter plots for WRF simulation (WRF-simulated) and combined model results (WRF-downscaled) air temperature at four local solar time of January 17. (Left side is WRF simulation and right side is combined model results. From up to down are the results of 02h, 08h, 14h and 20h, respectively.)

Although the spatial distribution of AWSs observation data interpolation results (GWR-interpolation) is not true value, it can represent the general distribution. Here, we use the GWR-interpolation as a benchmark to compare the spatial bias of WRF-simulated and WRF-downscaled. The spatial distribution of WRF-simulated, WRF-downscaled and GWR-interpolation of 02h and 14h are showed in Fig. 8 and Fig. 9. From Fig. 8 we know that WRF-simulated is generally greater than GWR-interpolation at 02h of local solar time, the spatial distribution of WRF-downscaled is closer to GWR-interpolation, and the WRF-downscaled can display more detail air temperature change caused by terrain change. Contrast with 02h, results of 14h (Fig. 9) show that WRF-simulated is generally lower than GWR-interpolation. The WRF-downscaled are like 02h, they are closer to observation interpolation results, and can display detail change cause by terrain. Through these spatial distributions, it can be found that the spatial distribution of the combined model prediction results is closer to interpolation results of observation data via GWR. The WRF-simulated temperature overall on the high side than observation data of ground stations at night, and overall low during the day time.

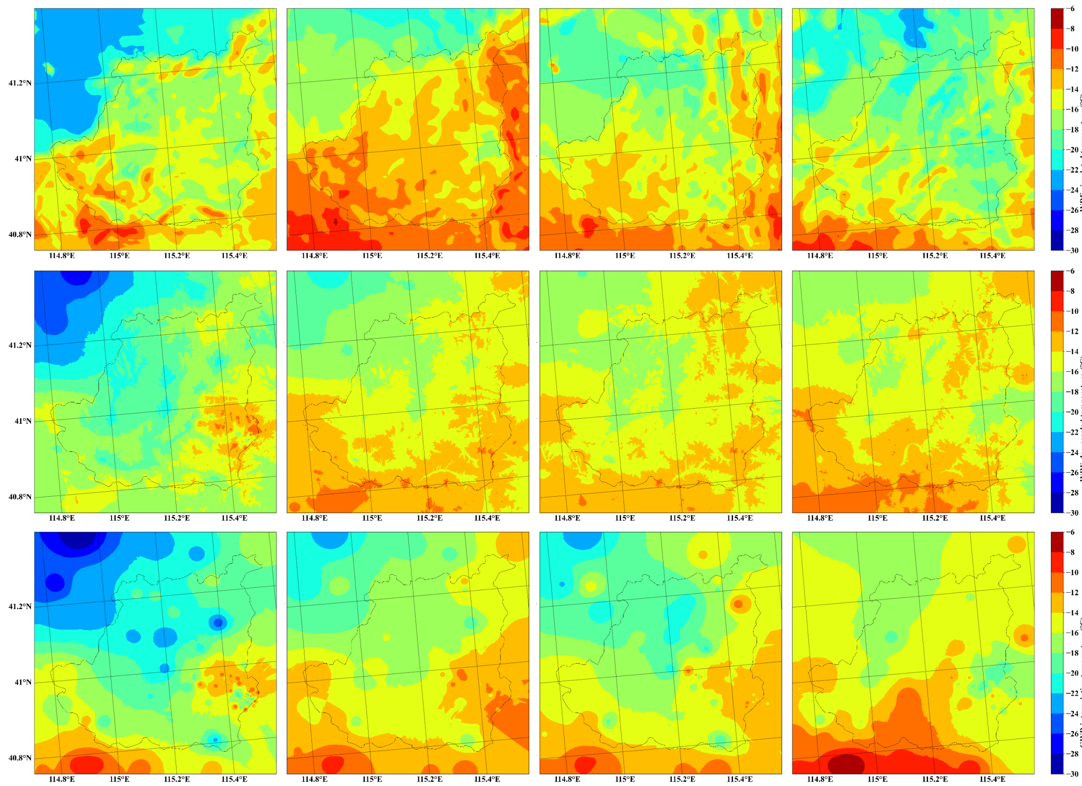

Fig. 8. Air temperature spatial distribution of WRF simulation (WRF-simulated), combined model downscaling results (WRF-downscaled) and observation data interpolation results (GWR-interpolation) at 02h. (From left to right are January 16, 17, 18 and 19, respectively. From upper to bottom are WRF-simulated, WRF-downscaled and GWR-interpolation, respectively.)

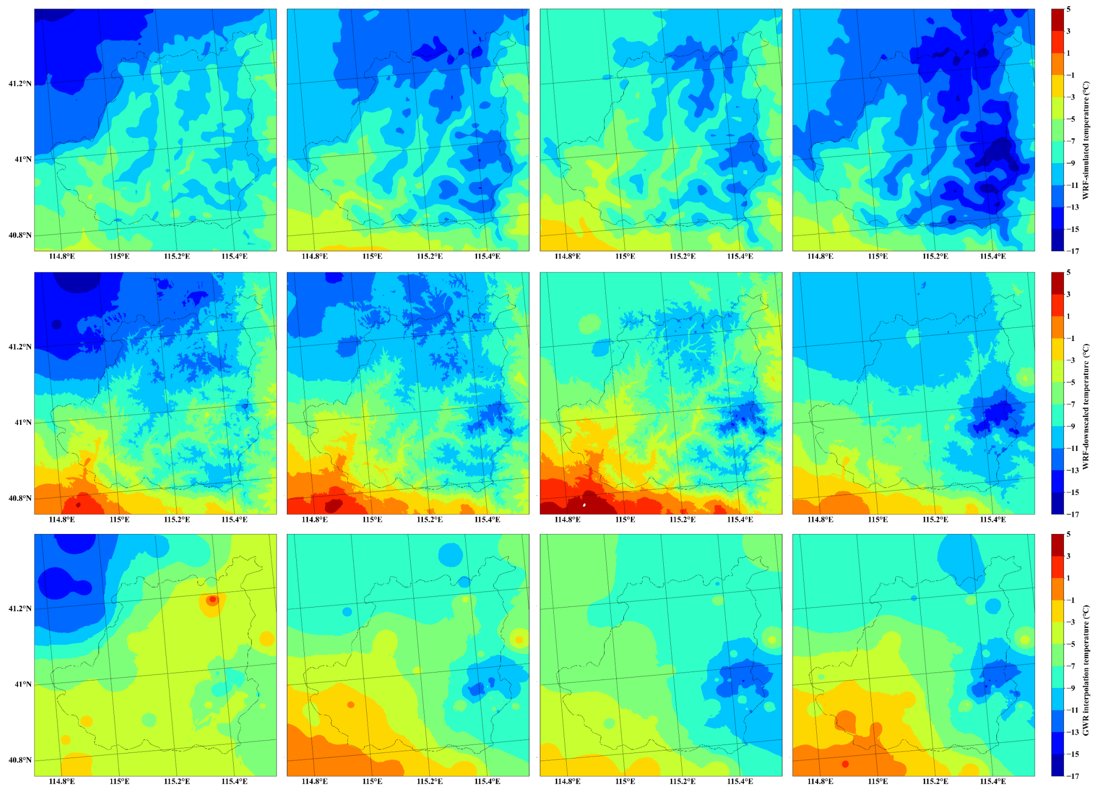

Fig. 9. Air temperature spatial distribution of WRF simulation (WRF-simulated), combined model downscaling results (WRF-downscaled) and observation data interpolation results (GWR-interpolation) at 14h. (From left to right are January 16, 17, 18 and 19, respectively. From upper to bottom are WRF-simulated, WRF-downscaled and GWR-interpolation, respectively.)

The spatial distribution of bias between combined model downscaling results (WRF-downscaled) and observation data GWR interpolation results (GWR-interpolation) of 02h and 14h are showed in Fig. 10.

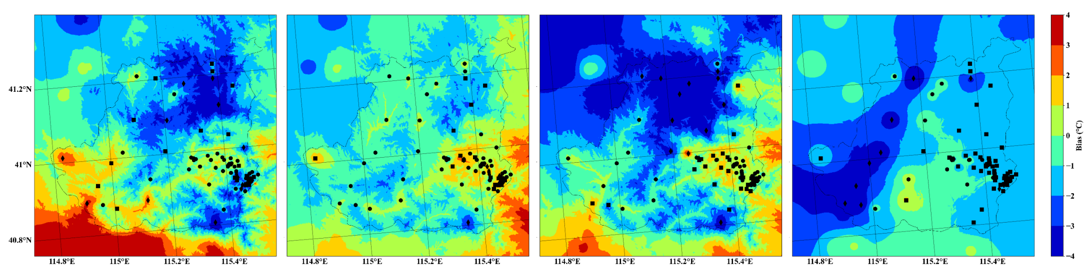

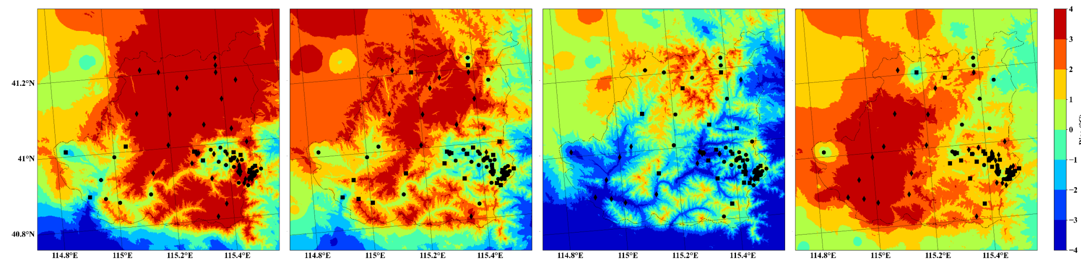

Fig. 10. Spatial distribution of air temperature bias between GWR-interpolation and WRF-downscaled. (From left to right are January 16, 17, 18 and 19, respectively. Upside is 02h, and downside is 14h. Circle dot represents MAE bias less than 1°C, square dot represents MAE bias between 1°C and 2°C, and diamond dot represents MAE of bias greater than 2°C.)

For 02h, the bias of most area is negative, its meaning WRF-downscaled is greater than GWR-interpolation. Combined with Fig. 8, we know that WRF simulation is generally greater than GWR-interpolation at 02h of local solar time. The generally negative bias is caused by this reason. The minimum bias areas locate in the northeast and southeast of the study area in January 16, 17 and 18, these areas have higher altitudes than other area. Contrary to those three days, the minimum bias area mainly locates in the southwest in January 19, and the southwest has lower altitude in the whole study area. We found that the bias of 02h mainly caused by temperature inversion, which common occurs at night. As shown in Fig. 11, observation temperature of AWSs increases with the increase of altitude in January 16, 17 and 18 (Under normal conditions air temperature usually decreases with altitude). However, WRF simulation fail to predict the temperature inversion. WRF simulation temperature of AWSs decreases with the increase of altitude. This leads to a bias increase with the altitude increase when temperature inversion occurs. Despite temperature inversion occurs in January 17, the top of inversion layer is about 1600m. The absolute bias of January 17 is lower than January 16 and January 18 in high altitude area by this reason. Different from the three days, inversion did not occur in January 19. The spatial pattern of January 19 is different from the other three days, the maximum of absolute bias occurs in low altitude area locate in the southwest of study area. In conclusion, temperature inversion affects the accuracy of temperature forecast at night. How to predict inversion and its intensity will help to improve the accuracy of air temperature prediction in mountain area at night.

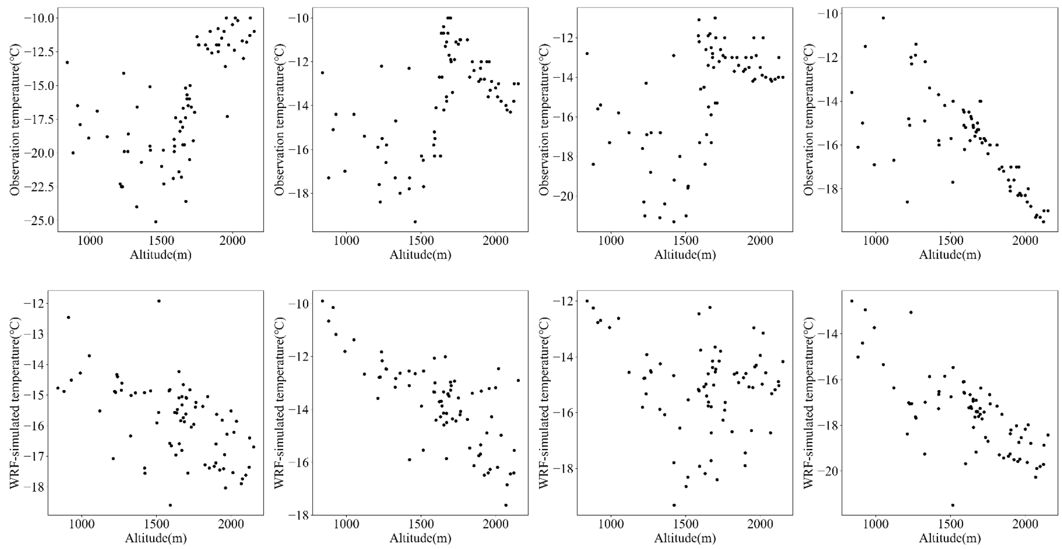

Fig. 11. Scatter plots of WRF simulation (WRF-simulated), observation temperature and altitude of all AWSs at 02h. (Upside is observation temperature, and downside is WRF simulation. From left to right are January 16, 17, 18 and 19, respectively.)

For 14h, the bias of most area is positive, its meaning WRF-downscaled is lower than GWR-interpolation. The generally positive bias is caused by the generally lower of WRF simulation than GWR-interpolation at 14h showed in Fig. 9. The MAE of WRF-simulated in 14h are 3.48℃, 3.39℃, 1.52℃, and 4.74℃ for January 16, 17, 18 and 19, respectively, as shown in Table 3. The MAE of 14h is significantly higher than at other times. After downscaling, the MAE of WRF-downscaled are 2.90℃, 1.95℃, 1.56℃, and 1.85℃ for January 16, 17, 18 and 19, respectively. There is a significant decrease in MAE for all forecast days at 14h. However, MAE is still relatively higher of 14h than other local solar times because the raw bias of WRF-simulated is too high at 14h. This leads to the overall high bias of the spatial distribution of WRF-downscaled at 14h. The combined downscaling model performance well when downscaling air temperature in this mountain area, however its accuracy depends on the accuracy of WRF simulation.

4. Conclusions

This study evaluated the use of combine GWR, bias correction, DTC model and MLR for WRF downscaling and correction in a mountain area. To reduce bias and improve the 2-m air temperature accuracy and spatial resolution of WRF simulation. The 2-m air temperature series predicted using the WRF model is first downscaling to 30-m from 1km grid via GWR. DTC model is used to fit the diurnal variation curve of air temperature in a day and using the curve to predict future 24-h hourly air temperature. The multiplicative correction is adopted to correct GWR downscaling results and to improve accuracy of daily mean air temperature of WRF simulation. MLR is employed in spatialization of all correction and DTC coefficients to train the relationship between these coefficients and slope, aspect, and altitude of study area. We tested this approach using ground observation data provided by the Hebei Meteorological Administration.

The combined downscaling model results (WRF-downscaled) can better express the detail features of air temperature than WRF simulation. Meanwhile, the influence of topography is reduced, and the forecasting accuracy is improved. The scheme was designed to work with hourly time scale, which are generally highly variable and more affected by weather conditions than daily or monthly means. The research presented here shows that air temperature of WRF simulation can be downscaled and corrected by this method, and the accuracy and spatial resolution of temperature forecast be improved in this area. Compare to WRF simulation, RMSE of WRF-downscaled decreased 1.01 ℃ at AWSs level and 0.80 ℃ at spatial level, and MAE decreased by 0.81 ℃ and 0.69 ℃ at two levels, respectively. Meanwhile, the correlation between WRF-downscaled and observation data (or observation data GWR interpolation results) is more well-fitted to the one-to-one line than WRF simulation. The spatial distribution of WRF-downscaled is closer to that of observation data GWR interpolation results than WRF simulation.

There are three major findings. First, multiplicative correction method is useful for correct WRF simulation air temperature, and the accuracy of this method is better to correct daily mean air temperature than hourly air temperature, meanwhile for short-term forecast (in this study is a day forecast) set n equals to one is better. Second, DTC model can represent most of the daily variations and its performance well when to forecast. Third, the proposed 2-m air temperature prediction model has high prediction accuracy and stability and provides a day-ahead high-resolution prediction, and is suitable for actual temperature production in this mountain area.

As the combined downscaling model in this paper does not require much time and computational resource to implement, and the data source is also easy to obtain, this methodology can easily be extended to other variables, regions, and numerical models. With additional data, slope, aspect, and land cover, it should be possible to improve spatialization of the models and overall model performance. The anticipated to further develop high spatial and temporal resolution temperature products across a large region of mountain area in the North China.

Despite the combined downscaling model performance well, there also some disadvantage, such as the smooth curve of DTC model is difficult to fit the sudden change of temperature. This kind of sudden change of temperature is not all random error, but it's really exists in diurnal temperature cycle. Meanwhile, temperature inversion has a great influence on the forecast of air temperature at night. To forecast this kind of sudden change and prediction and elimination of temperature inversion are not contain in this paper, it can be studied deeply in the follow-up research.

5. Acknowledgements

This study was supported by National Key R&D Program of China (No. 2018YFC1506801), S&T Program of Hebei (No. 19975414D), Postgraduate Research & Practice Innovation Program of Jiangsu Province (No. KYCX20_0931), and the Natural Science Foundation of China (No. 41871028).

References

Abdel-Aal, R.E., 2004. Hourly temperature forecasting using abductive networks. Engineering Applications of Artificial Intelligence. 17(5), 543-556.

Borrego, C., Monteiro, A., Pay, M.T., Ribeiro, I., Miranda, A.I., Basart, S., Baldasano, J.M., 2011. How bias-correction can improve air quality forecasts over Portugal. Atmospheric Environment. 45, 6629-6641.

Cheng, C.S., Li, G., Li, Q., Auld, H., 2008. Statistical downscaling of hourly and daily climate scenarios for various meteorological variables in South-central Canada. Theor. Appl. Climatol. 91, 129-147.

Cifuentes, J., Marulanda, G., Bello, A., Reneses, J., 2020. Air Temperature Forecasting Using Machine Learning Techniques: A Review Energies. 13, 4215. https://doi.org/10.3390/en13164215.

Ben-Nakhi, A.E., Mahmoud, M.A., 2004. Cooling load prediction for buildings using general regression neural networks. Energy Conversion and Management. 45, 2127-2141.

Caldwell, P., Chin, H.N.S., Bader, D.C., Bala, G., 2009. Evaluation of a WRF dynamical downscaling simulation over California. Climatic Change. 95, 499-521.

Chung, U., Seo, H.H., Hwang, K.H., Hwang, B.S., Choi, J., Lee, J.T., Yun, J. I., 2006. Minimum temperature mapping over complex terrain by estimating cold air accumulation potential. Agric. For. Meteorol. 137(1-2),15-24.

Dombaycı, Ö.A., Gölcü, M., 2009. Daily means ambient temperature prediction using artificial neural network method: A case study of Turkey. Renewable Energy. 34,1158-1161.

Duan, S.B., Li, Z.L., Wang, N., Wu, H., Tang, B.H., 2012. Evaluation of six land-surface diurnal temperature cycle models using clear-sky in situ and satellite data. Remote Sensing of Environment. 124, 15-25.

Duan, S.B., Li, Z.L., Tang, B.H., Wu, H., Tang, R., Bi, Y., Zhou, G., 2014. Estimation of diurnal cycle of land surface temperature at high temporal and spatial resolution from clear-sky. MODIS data. Remote Sens. 6, 3247-3262.

Fotheringham, A. S., Charlton, M., Brunsdon, C., 1997. Measuring spatial variations in relationships with geographically weighted regression. Springer, pp. 60-82.

Fotheringham, A.S., Oshan, T.M., 2016. Geographically weighted regression and multicollinearity: dispelling the myth. Journal of Geographical Systems, 18(4), 303-329.

Georganos, S., Abdi A.M., Tenenbaum, D.E., Kalogirou S., 2017. Examining the NDVI-rainfall relationship in the semi-arid Sahel using geographically weighted regression. Journal of Arid Environments. 146, 64-74.

Gholamnia, M., Alavipanah, S.K., Boloorani, A.D., Hamzeh, S., Kiavarz, M., 2017. Diurnal Air Temperature Modeling Based on the Land Surface Temperature. Remote Sens. 9, 915. https://doi.org/10.3390/rs9090915.

Gholamnia, M., Alavipanah, S.K., Boloorani, A.D., Hamzeh, S., Kiavarz, M., 2019. A new method to model diurnal air temperature cycle. Theoretical and Applied Climatology. 137, 229-238.

Hofer, M., Marzeion, B., Mölg, T., 2015. A statistical downscaling method for daily air temperature in data-sparse, glaciated mountain environments. Geoscientific Model Development. 8, 579-593.

Holden, Z.A., Abatzoglou, J.T., Luce, C.H., Baggett, L.S., 2011. Empirical downscaling of daily minimum air temperature at very fine resolutions in complex terrain. Agric. For. Meteorol. 151, 1066-1073.

Hu, L, Sun, Y., Collins, G., Fu, P., 2020. Improved estimates of monthly land surface temperature from MODIS using a diurnal temperature cycle (DTC) model. ISPRS Journal of Photogrammetry and Remote Sensing. 168, 131-140.

Ines, A.V.M., Hansen, J.W., 2006. Bias correction of daily GCM rainfall for crop simulation studies. Agric. For. Meteorol. 138, 44-53.

Jiang, Y., Yang, K., Shao, C., Zhou, X., Zhao, L., Chen, Y., Wu, H., 2021. A downscaling approach for constructing high-resolution precipitation dataset over the Tibetan Plateau from ERA5 reanalysis, Atmospheric Research, 256 105574.

Khosravi, Y., Lashkari, H., Asakereh, H., 2017. Spatial variability of water vapour in south and southwest of Iran. Mausam, 68, 9-22.

Konovalov, I.B., Beekmann, M., Meleux, F., Dutot, A., Foret, G., 2009. Combining deterministic and statistical approaches for PM10 forecasting in Europe. Atmospheric Environment. 43, 6425-6434.

Le Roux, R., Katurji, M., Zawar-Reza, P., Quénol, H., Sturman, A., 2018. Comparison of statistical and dynamical downscaling results from the WRF model. Environ. Model. Softw. 100, 67-73.

Li, S., Goel, L., Wang, P., 2016. An ensemble approach for short-term load forecasting by extreme learning machine. Applied Energy. 170, 22-29.

Mok, K.M., Miranda, A.I., Yuen, K.V., Hoi, K.I., Monteiro, A., Ribeiro, I., 2017. Selection of bias correction models for improving the daily PM10 forecasts of

WRF-EURAD in Porto, Portugal. Atmos. Pollut. Res. 8, 628-639.

Monteiro, A., Ribeiro, I., Tchepel, O., Sá, E., Ferreira, J., Carvalho, A., Martins, V., Strunk, A., Galmarini, S., Elbern, H., Schaap, M., Builtjes, P., Miranda, A., Borrego, C., 2013. Bias Correction Techniques to Improve Air Quality Ensemble Predictions: Focus on O3 and PM Over Portugal. Environmental Modeling & Assessment. 18, 533-546.

Neal, L.S., Agnew, P., Moseley, S., Ordóñez, C., Savage, N.H., Tilbee, M., 2014. Application of a statistical post-processing technique to a gridded, operational, air quality forecast. Atmospheric Environment. 98, 385-393.

Pierce, D.W., Cayan, D.R., Maurer, E.P., Abatzoglou, J.T., Hegewisch, K.C., 2015. Improved bias correction techniques for hydrological simulations of climate change. Journal of Hydrometeorology. 16, 2421−2442.

Reicosky, D.C., Winkelman, L.J., Baker, J.M., Baker, D.G., 1989. Accuracy of hourly air temperatures calculated from daily minima and maxima. Agric. For. Meteorol. 46, 193-209.

Schoof, J.T., Pryor, S.C., 2001. Downscaling temperature and precipitation: a comparison of regression-based methods and artificial neural networks. International Journal of Climatology. 21, 773-190. https://doi.org/10.1002/joc.655.

Silibello, C., D'Allura, A., Finardi, S., Bolignano, A., Sozzi, R., 2015. Application of bias adjustment techniques to improve air quality forecasts. Atmospheric Pollution Research, 6, 928-938.

Smith, D.M., Cusack, S., Colman, A.W., Folland, C.K., Harris, G.R., Murphy, J.M., 2007. Improved Surface Temperature Prediction for the Coming Decade from a Global Climate Model. Science. 317, 796-799.

Vigaud, N., Vrac, M., Caballero, Y., 2013. Probabilistic downscaling of GCM scenarios over southern India. International Journal of Climatology. 33, 1248-1263.

Viggiano, M., Busetto, L., Cimini D., Di Paola, F., Geraldi, E., Ranghetti, L., Ricciardelli, E., Romano, F., 2019. A new spatial modeling and interpolation approach for high-resolution temperature maps combining reanalysis data and ground measurements. Agric. For. Meteorol. 276-277, 107590.

Wang, J., Fonseca, R. M., Rutledge, K., Martín-Torres, J., Yu, J., 2020. A Hybrid Statistical-Dynamical Downscaling of Air Temperature over Scandinavia Using the WRF Model. Advances in Atomospheric Sciences. 37, 57-74.

Wang, K., Li, Y., Luo, Z., Yin, S., Chan, P.K., 2018. Harmonic analysis of 130-year hourly air temperature in Hong Kong: detecting urban warming from the perspective of annual and daily cycles. Clim. Dynam. 51, 613-625.

Wilby, R.L., Dawson, C.W., Barrow, E.M., 2002. SDSM - a decision support tool for the assessment of regional climate change impacts, Environmental Modelling & Software. 17, 145-157. https://doi.org/10.1016/S1364-8152(01)00060-3.

Wilczak, J., McKeen, S., Djalalova, I., Grell, G., Peckham, S., Gong, W., Bouchet, V., Moffet, R., McHenry, J., McQueen, J., Lee, P., Tang, Y., Carmichael, G.R., 2006. Bias-corrected ensemble and probabilistic forecasts of surface ozone over eastern north America during the summer of 2004. Journal of Geophysical Research: Atmospheres. 111(D23).

Xu, W., Liu, P., Cheng, L., Zhou, Y., Xia, Q., Gong, Y., Yini Liu, Y., 2021. Multi-step wind speed prediction by combining a WRF simulation and an error correction strategy. Renewable Energy. 163, 772-782.

Yan, D., Liu, T., Dong, W., Liao, X., Luo, S., Wu, K., Zhu, X., Zheng, Z., Wen, X., 2020. Integrating remote sensing data with WRF model for improved 2-m temperature and humidity simulations in China. Dynamics of Atmospheres and Oceans. 89, 101127.

Yi, C., Shin, Y., Roh, J.W., 2018. Development of an Urban High-Resolution Air Temperature Forecast System for Local Weather Information Services Based on Statistical Downscaling. Atmosphere. 9. 164.

Zhou, J., Chen, Y., Zhang, X., Zhan, W., 2013. Modelling the diurnal variations of urban heat islands with multi-source satellite data. Int. J. Remote Sens. 34 (21), 7568-7588.

Zhou, Q., Wang, C., Fang, S., 2019. Application of geographically weighted regression (GWR) in the analysis of the cause of haze pollution in China. Atmos. Pollut. Res. 10, 835-846.